4th IFAC Workshop on Distributed Estimation
and Control in Networked Systems
September 25-26, 2013. Rhine-Moselle-Hall, Koblenz, Germany

DisCoverage: From Coverage to Distributed Multi-Robot Exploration ⋆

D. Haumann * **V. Willert** * **K.D. Listmann** **

* *Institute of Automatic Control and Mechatronics, Technische Universität Darmstadt, Landgraf-Georg-Str. 4, 64283 Darmstadt, Germany* {dhaumann, vwillert}@rtr.tu-darmstadt.de.
** *ABB AG, Corporate Research, Wallstadter Str. 59, 68526 Ladenburg, Germany,* (kdl@ieee.org)

Abstract: DisCoverage transfers the well-known solution to the coverage problem to the exploration problem. Essentially, DisCoverage solves the multi-robot exploration problem through a spatially distributed optimization problem. Our contribution is a new objective function for DisCoverage based on the centroidal search. Each robot continuously creates and optimizes the proposed objective function, obtaining a gradient-based control law that leads into unexplored regions. A proof of convergence is given as well as a simulation and a statistical evaluation demonstrating DisCoverage.

Keywords: distributed control, distributed optimization, mobile robots, robot navigation, multi-robot exploration, dynamic coverage

1. INTRODUCTION

Motion coordination of mobile robots has received considerable amount of attention in the autonomous robotics community. Within the past decade the focus shifted from the single-robot to the multi-robot domain, stressing the need for distributed coordination techniques that enable a group of robots to act as a whole based on locally available information (Martínez et al., 2007). Examples are manifold and include consensus, flocking, sensor deployment, target tracking, and task allocation. Although these problems are in common need of distributed motion coordination techniques, individual solutions to these problems exist. Often the considered problem is solved isolated from solutions to related problems.

In particular, this observation holds for solutions to the coverage and the exploration problem. As noted by Burgard et al. (2005) the key problem in multi-robot exploration is to assign appropriate *target points* to each robot such that all robots simultaneously explore different regions of the environment. Therefore, existing exploration strategies traditionally apply a two-step approach: First, appropriate target points are chosen. Second, each robot plans a path with standard path planning algorithms (LaValle, 2006). Consequently, the difficulty of distributed multi-robot exploration lies in finding appropriate target points for each robot in a *distributed* manner. Typically, effective target point selection is achieved by casting the exploration task into a distributed optimization problem based on an appropriate objective function.

A vast amount of research on exploration exists that follows this two-step approach, focusing on different aspects. To name a few, Burgard et al. (2005) maximize the expected information gain, Fox et al. (2006) in particular solve the problem of Simultaneous Localization and Mapping (SLAM), Sheng et al. (2006) and Rooker and Birk (2007) focus on maintaining a communication network amongst the robots, and Wu et al. (2010) cluster the unknown space such that the robots evenly spread into the unknown environment.

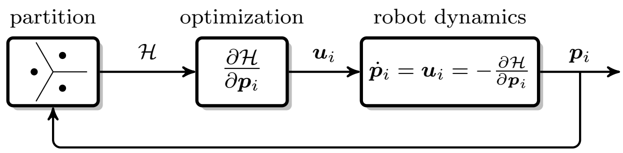

Fig. 1. Closed feedback loop (cf. Haumann et al. (2010))

Contrary to the two-step approach to multi-robot exploration, Cortés et al. (2005) provide a closed solution to the coverage problem with multiple robots. There, the steps of finding appropriate target points and path planning are merged. Consequently, the additional step of path planning is not needed. This is achieved by gradient-based motion control laws, as depicted in Fig. 1. Based on the Voronoi partition of the environment, the task of each robot is to maximize coverage in its own Voronoi cell. Maximizing coverage is achieved by the optimization of an objective function $\mathcal{H}$, resulting in gradient-based control inputs $\boldsymbol{u}_i$ that exclusively depend on information available in the respective Voronoi cell.

The significant property of the solution to the coverage problem in Fig. 1 is that it is spatially distributed over the Delaunay graph, which is dual to the Voronoi partition (de Berg et al., 2008). Once the partition is computed, which is possible distributively amongst Voronoi neighbors (Cao and Hadjicostis, 2003), the optimization and motion coordination is *fully distributed.* Martínez et al. (2007)

⋆ This work was gratefully supported by the German Research Foundation (DFG) within the GRK 1362 "Cooperative, Adaptive and Responsive Monitoring of Mixed Mode Environments".
⋆ Thanks to Lukas Klodt for his critical reviews.

provide a variety of motion coordination algorithms simply by modifying the objective function $\mathcal{H}$, with the most prominent one being the centroidal search.

Haumann et al. (2010) introduce *DisCoverage* as a paradigm to multi-robot exploration. In essence, the DisCoverage paradigm follows the closed feedback loop of the solution to the coverage problem in Fig. 1 by modifying the optimization problem such that the robots jointly explore the environment. Haumann et al. (2010) propose an objective function $\mathcal{H} = \sum_i \mathcal{H}_i$ consisting of the robot orientations δ_i defining the current moving direction, and distance costs to unexplored space. Each robot optimizes $\frac{\partial \mathcal{H}_i}{\partial \delta_i}$, i.e. its objective function $\mathcal{H}_i$ *with respect to its orientation* δ_i (instead of its position $\boldsymbol{p}_i$ as in Fig. 1) to obtain an optimal moving direction that quickly leads to unexplored space. Although the approach was extended to nonconvex environments and validated in lab experiments (Haumann et al., 2011), the proper choice of parameters and a formal proof of convergence are open issues.

In this paper we apply the DisCoverage paradigm again. However, this time we introduce an objective function $\mathcal{H}_{\text{discover}}$ that – being optimized with respect to the robot positions $\boldsymbol{p}_i$ as in Fig. 1 – provides a provably correct approach to distributed multi-robot exploration that closely follows the *limited centroidal search* as proposed by Cortés et al. (2005) for solving the coverage problem. We restrict the presented work to robots with single integrator dynamics exploring convex polygonal environments for clarity. It should be noted that the proposed method can be extended to system dynamics other than single integrator dynamics by following Bullo et al. (2009). In addition, it is possible to extend the work to nonconvex polygonal environments with several minor adjustments.

Other efforts have been made to combine coverage and exploration. Hussein and Stipanovic (2007) *dynamically cover* the entire search domain over time, which matches the idea of exploration. Although the authors provide a gradient-based control strategy, convergence cannot be guaranteed due to local minima. In that case, the strategy needs to be switched to a different coverage strategy. Closest to the DisCoverage approach proposed in this paper is the strategy by Bhattacharya et al. (2013). The authors follow the feedback loop in Fig. 1 by applying the *unlimited* centroidal search based on the Voronoi partition. If the centroid lies in already explored space, it is projected to the nearest location where the desired coverage level is not yet reached. Although this approach is provably correct, neither the centroid of an unlimited Voronoi cell nor its projection are optimal target points with respect to the exploration problem, since the centroid does not lie in unexplored space in most cases. Finally, Schwager et al. (2011) provide a unified approach to multi-robot deployment, but exploration is not considered.

The paper is structured as follows: Section 2 provides preliminaries and formally introduces the solution to the coverage problem and the problem statement. In Section 3 we apply the DisCoverage paradigm based on the coverage functional. This is achieved through an *integration range* and a modified density function. Further, we prove convergence. Section 4 shows simulation results and a statistical evaluation before we conclude in Section 5.

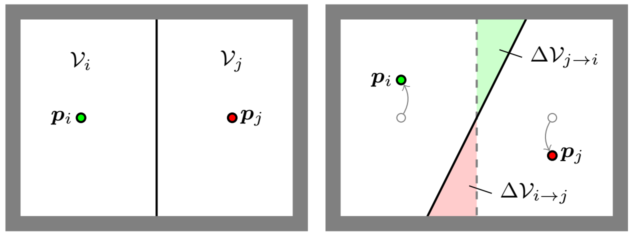

(a) Voronoi cells for 2 robots (b) Changed partition after Δt

Fig. 2. Exchanged map data amongst Voronoi neighbors

2. PROBLEM FORMULATION

2.1 Preliminaries

Although nonconvex polygonal environments with obstacles are supported with minor adjustments, we consider only *convex, obstacle-free* polygonal environments $\mathcal{Q} \subset \mathbb{R}^2$ for clarity. With $\partial\mathcal{Q}$ we denote the boundary of $\mathcal{Q}$. We assume *ideal measurements* within the radially limited *sensing range* $r \in \mathbb{R}_{>0}$. Any uncertainties in the robot positions and the sensor model are neglected, avoiding the problem of SLAM. Next, let $\mathcal{P} = \{\boldsymbol{p}_1, \ldots, \boldsymbol{p}_N\}$ be the configuration of N robots $\boldsymbol{p}_i \in \mathcal{Q}$. Define the Voronoi cells as $\mathcal{V}_i = \{\boldsymbol{q} \in \mathcal{Q} \mid \|\boldsymbol{q} - \boldsymbol{p}_i\|_2 \leq \|\boldsymbol{q} - \boldsymbol{p}_j\|_2, \forall j\}$ and let $\mathcal{V} = \{\mathcal{V}_1, \ldots, \mathcal{V}_N\}$ be the Voronoi partition. Further, define the $\bar{r}$-limited Voronoi cells as $\mathcal{V}_{i,\bar{r}} = \{\boldsymbol{q} \in \mathcal{V}_i \mid \|\boldsymbol{q} - \boldsymbol{p}_i\|_2 \leq \bar{r}\}$. We call the scalar $\bar{r} \in \mathbb{R}_{>0}$ *integration range*. We refer to robots with adjoining Voronoi cells as *neighbors* and assume *ideal, bidirectional communication* between neighbors. Further, neighbors communicate each other's position and exchange map data to account for the time-varying Voronoi cells according to Fig. 2. For $\Delta t \to 0$, neighbors i, j differentially exchange map data of the areas $\Delta\mathcal{V}_{i\to j}$. Last, define the δ-contraction of $\mathcal{Q}$ as $\mathcal{Q}_\delta = \{\boldsymbol{q} \in \mathcal{Q} \mid \inf_{\boldsymbol{q}' \in \partial\mathcal{Q}} \|\boldsymbol{q} - \boldsymbol{q}'\|_2 \geq \delta\}$.

2.2 Problem Description

We assume a homogeneous multi-robot system with a simple integrator dynamics

$$\dot{\boldsymbol{p}}_i = \boldsymbol{u}_i \tag{1}$$

for each robot, where $\boldsymbol{p}_i \in \mathcal{Q}$ denotes the position, and $\boldsymbol{u}_i \in \mathbb{R}^2$ the control input of robot i. Cortés et al. (2005) propose the r-limited centroidal search with sensing range r in terms of the *expected-value multicenter function*

$$\mathcal{H}_{\text{cover}}(\mathcal{P}) = \sum_{i=1}^{N} \int_{\mathcal{V}_i} f(\|\boldsymbol{q} - \boldsymbol{p}_i\|_2)\phi(\boldsymbol{q})d\boldsymbol{q}. \tag{2}$$

Therein, $f : \mathbb{R}_{\geq 0} \to \mathbb{R}_{\geq 0}$, $f(x) = x^2$ if $x \leq r$, and $f(x) = r^2$ if $x > r$, denotes the nondecreasing *performance function*. Increasing values f up to r^2 imply performance degradation. The *density function* $\phi(\boldsymbol{q})$ encodes a location dependent information gain at a point $\boldsymbol{q} \in \mathcal{Q}$. Cortés et al. (2005) show that minimizing (2) with respect to $\mathcal{P}$ yields N expected values, distributively optimizing the performance f in the r-limited Voronoi cells. Our idea is to modify (2) such that the optimization with respect to $\mathcal{P}$ distributively solves the exploration problem. The fundamental difference to existing exploration strategies is that each robot i optimizes the objective function $\mathcal{H}_{\text{cover}}$ in (2) with respect to its position $\boldsymbol{p}_i$ autonomously. Hence, all robots perform the optimization *in parallel* avoiding the two-step approach of the exploration problem. Distributed construction of a Voronoi cell is guaranteed as long as each robot is aware of the positions of its neighbors (Cao and Hadjicostis, 2003). Communication of robot positions and map information between neighbors (cf. Fig. 2) are the only requirements for our approach.

Focusing on exploration, we define $\mathcal{S}(t) \subseteq \mathcal{Q}$ as the explored space with $\partial\mathcal{S}(t) = \partial(\mathcal{S}(t) \setminus \partial\mathcal{Q})$ denoting the *frontier*. Let $\mathcal{S}_i(\mathcal{P}(t), t) = \mathcal{S}(t) \cap \mathcal{V}_i(\mathcal{P}(t))$, i.e., $\mathcal{S} = \cup_i \mathcal{S}_i$. Further, define $\partial\mathcal{S}_i(\mathcal{P}(t), t) = \partial\mathcal{S}(\mathcal{P}(t), t) \cap \mathcal{V}_i(\mathcal{P}(t))$ as the frontier in $\mathcal{V}_i(\mathcal{P}(t))$. For ease of notation, we occasionally omit the parameters $\mathcal{P}(t)$ and t and write $\mathcal{S}$, $\mathcal{S}_i$, $\partial\mathcal{S}_i$, and $\mathcal{V}_i$. How to achieve exploration will be subject of the next sections, and we conclude with the definition of our problem as follows:

Problem. Given a configuration $\mathcal{P} = \{\boldsymbol{p}_1, \ldots, \boldsymbol{p}_N\}$ of N robots in a convex polygonal environment $\mathcal{Q} \subset \mathbb{R}^2$, find an objective function $\mathcal{H}_{\text{discover}}$ of the form (2) to derive control laws $\boldsymbol{u}_i$ for (1) such that $\mathcal{S}(t) \to \mathcal{Q}$ as $t \to \infty$.

3. FROM COVERAGE TO DISCOVERAGE

Cortés et al. (2005) use the sensing range r to construct the r-limited Voronoi cells and a Gaussian density function $\phi(\boldsymbol{q})$. Instead, we introduce an *integration range* $\bar{r} \in \mathbb{R}_{>0}$ in addition to the sensing range to construct the $\bar{r}$-limited Voronoi cells $\mathcal{V}_{i,\bar{r}}$, and propose a density $\phi(\boldsymbol{q}, \partial\mathcal{S}_i(\mathcal{P}(t), t))$ as a function of the time-varying frontier $\partial\mathcal{S}_i$. Inserting the performance function f in (2), we denote $\mathcal{H}$ as

$$\mathcal{H}_{\text{discover}}(\mathcal{P}, \mathcal{S}) = \sum_{i=1}^{N} \int_{\mathcal{V}_{i,\bar{r}}} \|\boldsymbol{q} - \boldsymbol{p}_i\|_2^2 \phi(\boldsymbol{q}, \partial\mathcal{S}_i) d\boldsymbol{q} + R \quad (3)$$

with an additive term R. The idea is to find a density as a function of the time-varying frontier, such that the centroids of the gradient-based motion control laws

$$\dot{\boldsymbol{p}}_i = \boldsymbol{u}_i = -\frac{\partial\mathcal{H}_{\text{discover}}}{\partial\boldsymbol{p}_i}(\mathcal{P}, \mathcal{S}), \quad \text{for } i = 1, \ldots, N, \quad (4)$$

continuously approach the frontier, leading the robots into unexplored regions. Therefore, the next section first discusses the density before the gradient in (4) is given.

Remark 1. R in (3) accounts for the set $\mathcal{Q} \setminus \cup_i \mathcal{V}_{i,\bar{r}}$, where $\|\boldsymbol{q} - \boldsymbol{p}_i\|_2 > r$, and therefore $f(x) = r^2 = \text{const}$ from (2). This term vanishes in the derivative $\frac{\partial\mathcal{H}_{\text{discover}}}{\partial\mathcal{P}}$ and is therefore not further discussed (cf. Cortés et al. (2005)).

3.1 The Density Function

As a well-known fact, the objective function of the r-limited centroidal search along with the gradient-based motion control laws move the robots to locations with high density, maximizing coverage (Bullo et al., 2009). Therewith, it is fundamental that the density function ϕ is designed such that its values are maximal in the critical locations and monotonically decrease with increasing distance to the critical points.

In our case, the critical target points the robots need to reach are located on the frontier. Therefore, we define the density as a function of the time-varying frontier in terms of the Gaussian mapping $\phi : \mathcal{Q} \times \mathcal{Q} \to \mathbb{R}_{\geq 0}$,

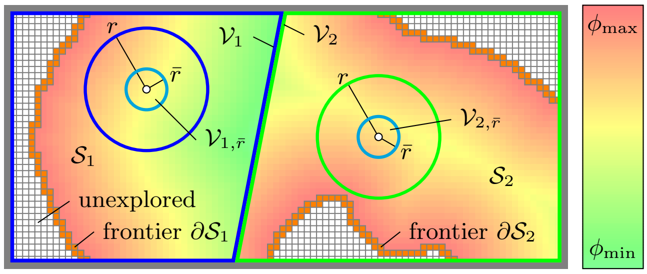

Fig. 3. Density function for 2 robots in the environment

$$\phi(\boldsymbol{q}, \partial\mathcal{S}_i) = \exp\left(-\frac{1}{2\sigma^2} \operatorname{dist}^2(\boldsymbol{q}, \partial\mathcal{S}_i)\right), \quad (5)$$

where in the convex case $\operatorname{dist}(\boldsymbol{q}, \partial\mathcal{S}_i) = \inf_{\boldsymbol{q}' \in \partial\mathcal{S}_i} \|\boldsymbol{q} - \boldsymbol{q}'\|_2$ computes the minimum Euclidean distance metric from $\boldsymbol{q}$ to the time-varying frontier $\partial\mathcal{S}_i(\mathcal{P}(t), t)$ through free space $\mathcal{S}_i$. Since the density function is a Gaussian, its value is highest on the frontier and monotonically decreases with increasing distance depending on the value of the standard deviation σ.

An example of the Gaussian density function (5) with $\sigma = 2\text{m}$ (m = meter) is shown in Fig. 3. Two robots are placed in a convex environment $\mathcal{Q}$ that is represented in terms of an occupancy grid map (Elfes, 1987; Moravec, 1988). Cells of the grid map are either *unexplored*, an *obstacle* on the boundary of $\mathcal{Q}$, or *free*. A cell on the boundary $\partial\mathcal{Q}$ of the environment switches its state from *unexplored* to *obstacle*, as soon as the cell intersects with a circle around the robot positions $\boldsymbol{p}_i$ defined by the sensing range r. A cell in the interior of $\mathcal{Q}$ switches its state from *unexplored* to *free*, if it is fully contained in one of the sensing circles. The frontier is defined by all unexplored cells adjoining free cells. The density decreases with larger distance and is depicted by the color gradient on a logarithmic scale.

Remark 2. (Relation to the distance transform). The computation of the weights of all points $\boldsymbol{q}$ in the explored region $\mathcal{S}_i$ relies on the distance from each $\boldsymbol{q}$ to the frontier $\partial\mathcal{S}_i$ in a Voronoi cell $\mathcal{V}_i$. Interestingly, this equals the distance transform known in image processing (e.g., Fabbri et al. (2008)), except that the distance is computed with respect to the frontier instead of the obstacles.

3.2 Building the Partial Derivative

Cortés et al. (2002) and Pimenta et al. (2008) consider time-varying density functions $\phi(\boldsymbol{q}, t)$ for target tracking. As a consequence, the control laws depend on the dynamics of the centroid of the r-limited Voronoi cells, which in turn depends on $\phi(\boldsymbol{q}, t)$. This dependency is required, since if the dynamics of $\phi(\boldsymbol{q}, t)$ is ignored, convergence and thus successful target tracking cannot be achieved.

In our case, the density function $\phi(\boldsymbol{q}, \partial\mathcal{S}_i(\mathcal{P}(t), t))$ in (5) does not explicitly depend on time. Instead, it depends on the state of the frontier $\partial\mathcal{S}_i(\mathcal{P}(t), t)$ in the Voronoi cell $\mathcal{V}_i(\mathcal{P}(t))$. This in turn implies that the frontier $\partial\mathcal{S}_i$ is constant over time if the robots do not move, i.e., if $\dot{\mathcal{P}} = \mathbf{0}$. Considering moving robots, the density in a Voronoi cell changes only in two cases: First, the robot moves into unexplored regions of the environment and consequently pushes back the frontier. Second, the partition changes such that parts of the frontier are assigned from Voronoi

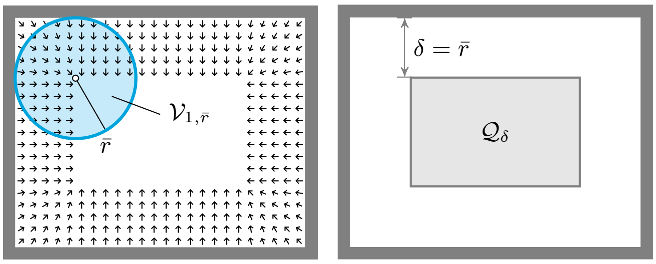

(a) vector field for $\phi = \text{const}$ (b) δ-contraction $\mathcal{Q}_\delta$ for $\delta = \bar{r}$

Fig. 4. Fully explored, convex environment $\mathcal{Q}$ with constant density. The boundary acts as repulsive force. Legend: ∘ robot position, — integration range $\bar{r}$, cell resolution $0.2\text{m} \times 0.2\text{m}$.

cell $\mathcal{V}_i$ to $\mathcal{V}_j$. With this background, it is not crucial to model the dynamics of the density function in the gradient (4). Therefore, we formulate the following assumption.

Assumption 3. Building the partial derivative of (3), the density ϕ can be modeled as a quasi-stationary function.

Under Assumption 3, one obtains the well-known gradients

$$\frac{\partial \mathcal{H}_{\text{discover}}}{\partial \boldsymbol{p}_i}(\mathcal{P}, \mathcal{S}) = k_i(\boldsymbol{p}_i - \text{CM}_\phi(\mathcal{V}_{i,\bar{r}})), \tag{6}$$

for each robot $i = 1, \ldots, N$ (Cortés et al., 2005). Therein, $k_i \in \mathbb{R}_{>0}$ denotes a positive gain, and the center of mass $\text{CM}_\phi(\mathcal{V}_{i,\bar{r}})$ denotes the weighted centroid of the $\bar{r}$-limited Voronoi cell $\mathcal{V}_{i,\bar{r}}$. Obviously, the negative gradient points straight from the robot position into the centroid, which reflects the desired behavior in (4). Although $\mathcal{H}_{\text{discover}}$ in (3) is defined over $\mathcal{Q}$, the partial derivatives (6) solely depend on $\boldsymbol{p}_i$ and $\mathcal{V}_{i,\bar{r}}$. Consequently, the computation of the partial derivatives is *fully distributed.*

3.3 Choice of Integration and Sensing Range

In addition to the density (5), the objective function $\mathcal{H}_{\text{discover}}$ in (3) depends on the integration range $\bar{r}$ which defines the $\bar{r}$-limited Voronoi cells $\mathcal{V}_{i,\bar{r}}$ in the Voronoi cell $\mathcal{V}_i$. The $\bar{r}$-limited Voronoi cells $\mathcal{V}_{i,\bar{r}}$ form the base for computing the motion control laws (4) through the partial derivatives (6). In the following, we examine the impact of the integration range $\bar{r}$ on the motion control laws $\boldsymbol{u}_i$ and the sensing range r, and therefore the entire exploration process. Based on examples, we deduce general upper and lower bounds for the integration and sensing range.

A good understanding of the impact of the integration range $\bar{r}$ is obtained by considering an explored, convex environment $\mathcal{Q}$ with a single robot and constant density $\phi_{\text{const}} = 1$ as shown in Fig. 4. In Fig. 4a the vector field is shown for the robot with an integration range of $\bar{r} = 1\text{m}$. The normalized gradients are computed by applying (6) to (4) in each cell of the explored environment. Obviously, the boundary acts as repulsive force such that all trajectories lead into an invariant set in $\mathcal{Q}$ that is defined by all points $\boldsymbol{q} \in \mathcal{Q}$ whose distance to the boundary $\partial\mathcal{Q}$ is greater than or equal to the integration range $\bar{r}$. This is formalized as follows.

Theorem 4. Given a single robot in $\boldsymbol{p}_1 \in \mathcal{Q}$ with $\bar{r}$-limited Voronoi cell $\mathcal{V}_{1,\bar{r}}$, integration range $\bar{r}$, and a constant density ϕ, all gradients (4) are zero in the δ-contraction $\mathcal{Q}_{\delta=\bar{r}}$ of $\mathcal{Q}$, which defines an invariant set. All negative gradients in (4) for $\boldsymbol{p}_1 \in \mathcal{Q} \setminus \mathcal{Q}_\delta$ point towards $\mathcal{Q}_\delta$.

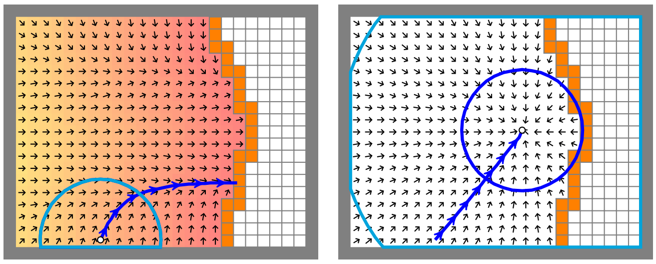

(a) preview of $\boldsymbol{p}_i(t)$ for $\bar{r} = 1\text{m}$ (b) $\boldsymbol{p}_i(t)$ for $\bar{r} = 3\text{m}$ and $r = 1\text{m}$

Fig. 5. Vector field for a convex environment with a single robot. Legend: ∘ robot position, — integration range $\bar{r}$, — sensing range r, → trajectory, cell resolution $0.2\text{m} \times 0.2\text{m}$.

Proof. If $\boldsymbol{p}_1 \in \mathcal{Q}_\delta$, the $\bar{r}$-limited Voronoi cell $\mathcal{V}_{1,\bar{r}}$ is radially unbounded. In this case, the centroid $\text{CM}_\phi(\mathcal{V}_{1,\bar{r}})$ lies in $\boldsymbol{p}_1$, and the gradients in (6) vanish. If $\boldsymbol{p}_1 \in \mathcal{Q} \setminus \mathcal{Q}_\delta$, the $\bar{r}$-limited Voronoi cell $\mathcal{V}_{1,\bar{r}}$ intersects with the boundary. In this case, the centroid $\text{CM}_\phi(\mathcal{V}_{1,\bar{r}})$ does not equal $\boldsymbol{p}_1$. Instead, it is pushed away from the boundary towards $\mathcal{Q}_\delta$. Bullo et al. (2009) prove that the gradients in (4) point straight from $\boldsymbol{p}_1$ into the centroid. Hence, trajectories starting in $\mathcal{Q} \setminus \mathcal{Q}_\delta$ approach $\mathcal{Q}_\delta$. □

Theorem 4 is an inherent property of the limited centroidal search (Bullo et al., 2009). The δ-contraction of $\mathcal{Q}$ is also known as *growing of obstacles* in robotics for collision-free path planning (Udupa et al., 1977; Lozano-Pérez and Wesley, 1979). The invariant set, where all gradients are zero, is equal to $\mathcal{Q}_\delta$ for $\delta = \bar{r}$ as shown in Fig. 4b. Consequently, the integration range can be thought of as a safety distance to the boundary. This further allows for a physical interpretation: When using real robots with physical diameter $\text{diam}_{\text{robot}}$ and dynamics (4), the integration range $\bar{r}$ must satisfy the lower bound

$$\bar{r} \geq \bar{r}_{\min} = \frac{1}{2}\,\text{diam}_{\text{robot}}\,. \tag{7}$$

If (7) is violated, the risk of colliding with the environment rapidly increases with decreasing integration range.

Unfortunately, (7) does not strictly hold for non-uniform densities such as (5), since higher densities may shift the centroid closer to the boundary depending on the slope of the density. Hence, the distance from the centroid to the boundary may be less than $\bar{r}$. Thus, applying Theorem 4 for non-uniform densities, (7) imposes only a necessary condition, but it is not sufficient to avoid collisions. Nevertheless, the δ-contraction can still be regarded as an approximate safety distance. This is depicted in Fig. 5a for a single robot in a partially explored convex environment $\mathcal{Q}$. In line with Fig. 3, the density is illustrated through the color gradient. Despite the non-uniform density, the trajectory of the robot still adheres to the safety distance of $\bar{r} = 1\text{m}$, finally approaching unexplored space.

Next to the lower bound $\bar{r}_{\min}$ of the integration range, we want to find an upper bound $\bar{r}_{\max}$. Closely investigating Fig. 5b reveals that too large values for $\bar{r}$ result in trajectories that all lead into a single time-invariant equilibrium point. In fact, for $\bar{r} \to \text{diam}\,\mathcal{Q}$, the limited

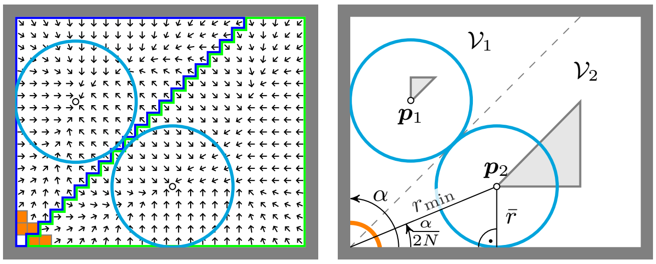

(a) $\partial\mathcal{V}_i$ acts as repulsive force (b) minimum sensing range $r_{\min}$

Fig. 6. $r_{\min}$ in dependence of N and the interior angle α

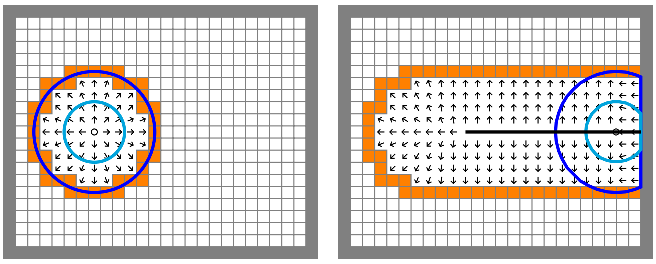

(a) Unstable equilibrium point (b) — unstable invariant set

Fig. 7. Unstable equilibrium points and invariant sets

centroidal search equals the unlimited centroidal search (Cortés et al., 2004), which is known to maximize coverage for the entire convex domain and therefore not suited for exploration. This also becomes clear by recognizing that the sensing range of $r = 1$m is not sufficient to explore new parts of the environment in Fig. 5b. From Fig. 4 and Theorem 4, it can be concluded that the δ-contraction of $\mathcal{Q}$ can be interpreted in terms of a defensive approximation of the *reachability set* for $\delta = \bar{r}$. The reachability set $\mathcal{Q}_\delta$ contains all points that can safely be reached while strictly maintaining the safety distance δ to the boundary $\partial\mathcal{Q}$. Increasing values for the integration range $\bar{r}$ push the robots further away from the boundary $\partial\mathcal{Q}$. Finally, a value $\delta_{\max}$ exists such that the reachability set $\mathcal{Q}_\delta$ degenerates into a single line or a point. The δ-contraction of $\mathcal{Q}$ for $\delta > \delta_{\max}$ yields an empty set $\mathcal{Q}_\delta = \emptyset$. Therefore, if a robot should be able to navigate in the environment $\mathcal{Q}$, the condition

$$\bar{r} \leq \bar{r}_{\max} = \delta_{\max} \tag{8}$$

must hold. Interestingly, $\mathcal{Q}_{\delta=\delta_{\max}}$ equals the paths defined by the generalized Voronoi partition (Latombe, 1991).

Next, we give a lower bound $r_{\min}$ for the sensing range r. To this end, we first note that the boundary $\partial\mathcal{V}_i$ of a Voronoi cell $\mathcal{V}_i$ acts as repulsive force exactly the same as the boundary $\partial\mathcal{Q}$ of the environment, see Fig. 6a. It follows that the minimum sensing range depends on the partition, the number of robots and the smallest interior angle α of the polygonal environment.

Theorem 5. (Lower bound for the sensing range r). Given N robots with integration range $\bar{r} > \bar{r}_{\min}$. Denote with α the smallest interior angle of the convex polygonal environment $\mathcal{Q}$. The minimum sensing range $r_{\min}$ required to explore $\mathcal{Q}$ is defined by

$$r_{\min} = \frac{\bar{r}}{\sin(\frac{\alpha}{2N})}. \tag{9}$$

Proof. Since the boundary of the Voronoi cell acts as repulsive force, consider the Voronoi cell $\mathcal{V}_i$ of a single robot. Therein, the reachability set is defined by the δ-contraction of the Voronoi cell $\mathcal{V}_i$ (cf. Fig. 6b). The interior angle $\frac{\alpha}{2N}$ in the Voronoi cell along with the minimum sensing range $r_{\min}$ and the integration range $\bar{r}$ define a right triangle. Using the sine function, one obtains $r_{\min}$ as hypotenuse. □

According to condition (9) in Theorem 5, the sensing range r must satisfy $r \geq r_{\min}$ to allow for complete exploration of the environment. Based on the discussion in this section, we sum up the results as follows.

Corollary 6. (Choice of integration and sensing range). Let $\mathcal{Q}$ be a convex environment. Then, the entire environment can be explored over time if the integration range $\bar{r}$ and the sensing range r of the robots satisfy (7) according to Theorem 4, and (9) of Theorem 5, respectively.

3.4 The Separatrix: Unstable Invariant Sets

The density function (5) assigns decreasing real values to each $\boldsymbol{q}$ with increasing distance to the frontier. However, considering that the frontier may have arbitrarily curved shapes during the exploration, the non-uniform weights in the explored parts $\mathcal{S}_i$ of the respective Voronoi cell $\mathcal{V}_i$ of the environment $\mathcal{Q}$ introduce multiple maxima and minima, where

$$\frac{\partial\mathcal{H}_{\text{discover}}}{\partial\boldsymbol{p}_i}(\mathcal{P},\mathcal{S}) = \mathbf{0} \tag{10}$$

holds. As frequently discussed in the solution to the coverage problem (Bullo et al., 2009), the objective function $\mathcal{H}_{\text{cover}}$ exhibits its minima for centroidal Voronoi configurations $\mathcal{P}$, maximizing coverage. However, (10) imposes only a necessary condition for a minimum, implying that a configuration $\mathcal{P}$ may represent a maximum. A maximum is the worst case for a centroidal Voronoi configuration $\mathcal{P}$, since the gradients are zero. Consequently, the robots remain at their position forever without moving to unexplored regions.

In fact, these worst-case situations appear frequently in the proposed approach to multi-robot exploration, as Fig. 7 shows for a single robot with integration range $\bar{r} = 0.5$m and sensing range $r = 1$m. In Fig. 7a, the vector field is shown for a single robot in an unknown environment right after mapping the surrounding area for the first time. Obviously, the gradient in the robot position is zero, and all other gradients in the explored region point away from the robot to the frontier. Hence, the robot is positioned in a maximum of the objective function $\mathcal{H}_{\text{discover}}$, which is equal to an unstable equilibrium point from a controls perspective. Theoretically, the robot stays in this position forever, and a random infinitesimal small perturbation needs to be added to the gradient to continue exploration. In Fig. 7b, the robot continued the exploration to the east, finally arriving at the boundary $\partial\mathcal{Q}$ of the environment. This time, the vector field reveals an invariant set in the shape of a line instead of a single equilibrium point. Analog to the circular case, all other gradients point towards the frontier, therefore the invariant set is unstable.

From a mathematical point of view, these unstable invariant sets can be detected by checking whether the Hessian matrix of $\mathcal{H}_{\text{discover}}$ with respect to a robot position $\boldsymbol{p}_i$ is negative definite. However, it is much more easy to detect this case according to the following observation.

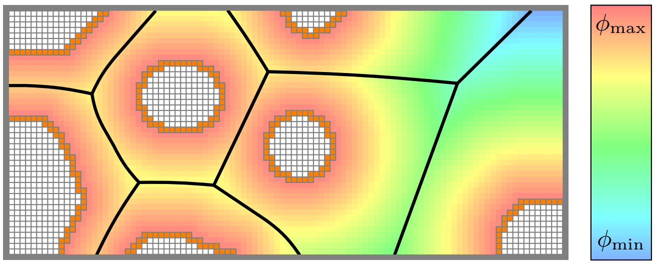

Fig. 8. Separatrix of the vector field, keeping maximum distance to the frontier.

Corollary 7. (Leaving unstable invariant sets).
If condition (10) holds, i.e., the gradient of robot i is $\mathbf{0}$, and if there still exists a frontier $\partial\mathcal{S}_i$ in the Voronoi cell $\mathcal{V}_i$ of the robot, then the robot is located in the unstable invariant set and an arbitrary perturbation must be added to the gradient for the robot to leave the invariant set and continue exploration.

Before further analyzing convergence properties of DisCoverage, we take a closer look at Fig. 8. Therein, all points in the unstable invariant set form the separatrix, highlighted by the solid line in the explored regions. The vectors are omitted for clarity. Interestingly, the separatrix appears to be defined in line with the generalized Voronoi partition, except that the distance is maximized with respect to the frontier instead of to the boundary $\partial\mathcal{Q}$. Thereafter, the separatrix equals the set defined by the maximum-clearance road maps in robot navigation (LaValle, 2006).

3.5 Proof of Convergence

According to the problem formulation in Section 2, the exploration process is complete if $\mathcal{S}(t) \to \mathcal{Q}$ as t approaches ∞. Since the density function is constructed such that it is maximal on the frontier and monotonically decreases with increasing distance to the frontier, the following theorem states that the $\bar{r}$-limited centroidal search, denoted by the objective function (3) together with the gradient-based motion control laws (4), moves the robots into regions with maximum density, resulting in a $\bar{r}$-limited centroidal Voronoi configuration.

Theorem 8. (Frontier-based centroidal search). Let $\mathcal{Q}$ denote a convex polygonal environment and let $\mathcal{S}$ denote the explored region in $\mathcal{Q}$. Let $\mathcal{P} = \{\boldsymbol{p}_1, \dots, \boldsymbol{p}_N\}$ be the configuration of N robots in $\mathcal{S}$ with integration range $\bar{r}$, and denote with $\mathcal{V} = \{\mathcal{V}_1, \dots, \mathcal{V}_N\}$ the Voronoi partition of $\mathcal{S}$ for $\mathcal{P}$. Then, applying (3) and (4) results in a $\bar{r}$-limited centroidal Voronoi partition for $t \to \infty$.

Proof. Building the time-derivative of (3) and inserting (4) yields

$$\begin{aligned}\dot{\mathcal{H}}_{\text{discover}}(\mathcal{P},\mathcal{S}) &= \sum_{i=1}^{N} \frac{\partial \mathcal{H}_{\text{discover}}}{\partial \boldsymbol{p}_i}(\mathcal{P},\mathcal{S})\dot{\boldsymbol{p}}_i \\ &= -\sum_{i=1}^{N} \left\| \frac{\partial \mathcal{H}_{\text{discover}}}{\partial \boldsymbol{p}_i}(\mathcal{P},\mathcal{S}) \right\|_2^2 \qquad (11)\end{aligned}$$

under Assumption 3. The partial derivatives of $\mathcal{H}_{\text{discover}}$ with respect to the robot positions $\boldsymbol{p}_i$ are given by (6). Inserting (6) into (11) is equivalent to

$$\dot{\mathcal{H}}_{\text{discover}}(\mathcal{P},\mathcal{S}) = -k_p \sum_{i=1}^{N} \|\boldsymbol{p}_i - \text{CM}_\phi(\mathcal{V}_{i,\bar{r}})\|_2^2 \le 0 \qquad (12)$$

for a positive gain k_p. Obviously, (3) decreases over time since the sum of squares as well as k_p in (12) are nonnegative. Applying the Krasovskii-LaSalle invariance principle (Khalil, 2001), the robots move to the largest invariant set, which equals the set of all $\bar{r}$-limited centroidal Voronoi configurations. □

With the help of Corollary 6 and 7, and Theorem 8, we next give a proof of convergence for the DisCoverage-based exploration approach.

Theorem 9. (Proof of convergence). Let $\mathcal{Q}$ denote a convex environment and let $\mathcal{S}$ denote the explored region in $\mathcal{Q}$. Let $\mathcal{P} = \{\boldsymbol{p}_1, \dots, \boldsymbol{p}_N\}$ be the configuration of N robots in $\mathcal{S}$ and denote with $\mathcal{V} = \{\mathcal{V}_1, \dots, \mathcal{V}_N\}$ the Voronoi partition of $\mathcal{S}$ for $\mathcal{P}$. Then, if $\bar{r} \ge \bar{r}_{\min}$ and $r \ge r_{\min} \ge \bar{r}$ holds and applying Corollary 7, continuous minimization of (3) and applying the motion control laws (4) solve the multi-robot exploration problem and $\mathcal{S}(t) \to \mathcal{Q}$ for $t \to \infty$.

Proof. Applying Corollary 6 and 7, the lower bound $\bar{r}_{\min}$ for the integration range $\bar{r}$ results in trajectories that approach the frontier, converging to a $\bar{r}$-limited centroidal Voronoi configuration as stated by Theorem 8. Since for the sensing range $r \ge r_{\min}$ holds, the frontier is within sensing range r and therefore pushed back, which in turn changes the density function $\phi(\boldsymbol{q}, \partial\mathcal{S}_i)$. Therewith, the $\bar{r}$-limited centroidal Voronoi configuration is never reached and the exploration continues until the entire environment is explored. □

In line with the solution to the coverage problem by Cortés et al. (2005), the optimization of the DisCoverage approach follows exactly the closed feedback loop in Fig. 1 with $\mathcal{H} = \mathcal{H}_{\text{discover}}$. The partition is defined by the Voronoi partition $\mathcal{V}$, the optimization by the density function (5) and the objective function (3), and the robot dynamics by the motion control laws (4) and (6).

4. RESULTS

We demonstrate DisCoverage in a rectangular environment $\mathcal{Q}$ of size 15m × 10m with $N = 3$ robots as shown in Fig. 9. The cell resolution of the grid map is set to 0.2m × 0.2m. The integration range is set to $\bar{r} = 0.5$m. Inserting $N, \bar{r}$ and the minimum interior angle $\alpha = \frac{\pi}{2}$ into (9) yields a minimum sensing range of $r_{\min} \approx 1.93$m. Satisfying Theorem 5, we set the sensing range to $r = 2\text{m} > r_{\min}$. The simulation is performed in the DisCoverage exploration framework (Haumann, 2013), which provides a discrete-time implementation of the proposed approach. Initially, the entire scene is unexplored. After 30 iterations, the robots spread into different directions, exploring unknown space in Fig. 9a. In addition to the trajectories, the integration range, the Voronoi cells as well as the vector fields of *free* grid cells in the respective Voronoi cells are visualized. The exploration proceeds over time (cf. Fig. 9b). Whenever no frontier cells are left in a Voronoi cell, i.e., $\partial\mathcal{S}_i = \emptyset$, a robot is said to be *unemployed*. In this case, the density ϕ is set to a constant value of one, and the robot falls back to the unlimited centroidal search in its Voronoi cell $\mathcal{V}_i$ (Cortés et al., 2004). The unlimited centroidal search equals setting the integration range $\bar{r}$ to ∞, meaning that the robot always integrates over the entire Voronoi cell $\mathcal{V}_i$ in (6). This effect can be observed in Fig. 9c for the robot in the upper right corner. Therein, all trajectories in the Voronoi cell point into one single equilibrium point. The exploration continues, until the entire environment is explored after 95 iterations as depicted in Fig. 9d.

Fig. 10 shows statistics for a sample size of 1000 simulation runs for the scene in Fig. 9. Each run starts with randomly generated initial robot positions. The number of iterations is displayed on the horizontal axis. The vertical axis shows the exploration progress in percent. A value of 100% implies that all grid cells are explored. Each iteration vertically shows a box plot: the ±25% band around the median represent 500 of the 1000 runs. The 'best case' corresponds to the maximum of the explored space in percent in each iteration, while the 'worst case' corresponds to the minimum.

In addition to the median, the mean and standard deviation of the iterations needed to explore 90%, 95%, 98% and 100% are depicted horizontally.

The slope of the exploration progress decreases with increasing number of iterations. This can be explained by observing that robots get unemployed during the exploration process. As already discussed based on Fig. 9c, an unemployed robot falls back to the unlimited centroidal search and therefore does not contribute to the exploration. Fig. 10 includes the statistics about how many robots are *unemployed* on average (in percent). Statistically, the unemployment decreases from iteration 88 to iteration 150, since an increasing number of simulation runs already explored 100% of $\mathcal{Q}$. That is, if a simulation run already finished exploration, all robots are counted as *employed* robots as they are open for new tasks.

Finally, Fig. 10 also shows the time-optimal case introduced by Frank et al. (2010). In short, the time-optimal case defines a lower bound of the iterations needed to explore an unknown environment.

5. CONCLUSION

In conclusion, this paper introduced a new approach to multi-robot exploration in line with the DisCoverage paradigm: Based on the elegant solution to the coverage problem, the limited centroidal search is modified to facilitate multi-robot exploration. To this end, an integration range was introduced and the density was defined as a function of the frontier. DisCoverage is fully distributed in terms of the gradient-based feedback loop in Fig. 1. The advantages to existing exploration strategies are as follows: First, distributed coordination is an inherent property because each robot solely relies on information available in its Voronoi cell. Second, due to the gradient-based motion control laws, an additional path planning step is not needed. An interpretation of the integration range in terms of a safety distance as well as lower and upper bounds were given, allowing for a formal proof of convergence. Further, the relation of DisCoverage to the method "growing of obstacles" as well as to the distance transform and the generalized Voronoi partition was given.

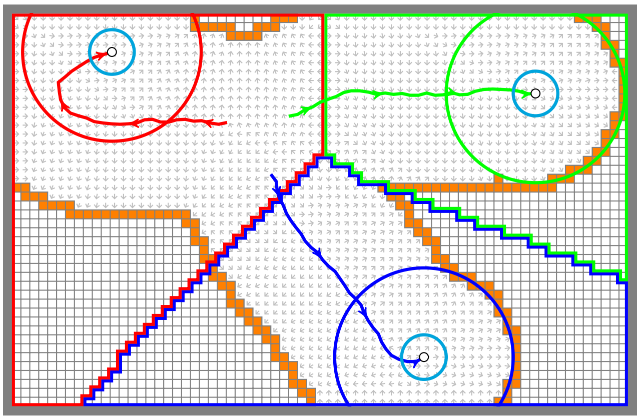

(a) Scene after 30 iterations

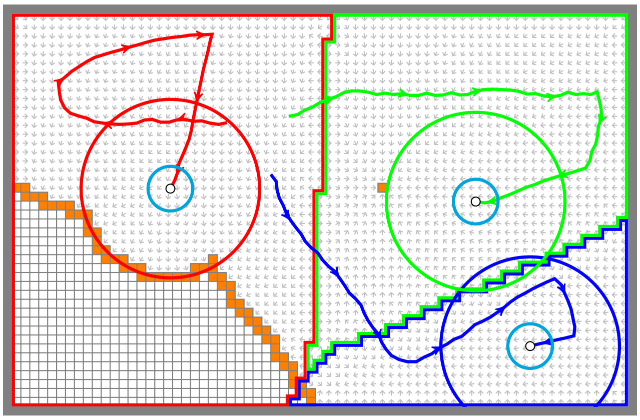

(b) Scene after 60 iterations

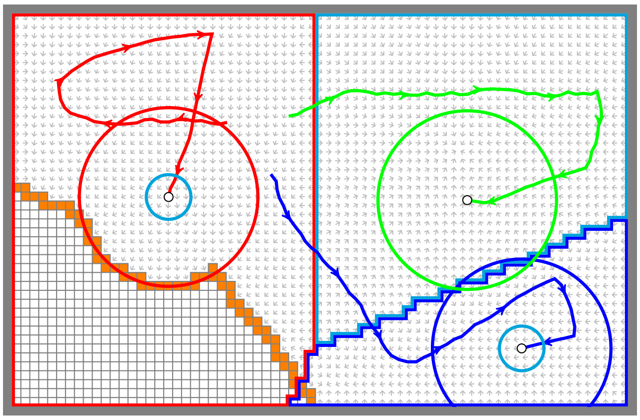

(c) Scene after 61 iterations

(d) Final configuration after 95 iterations

Fig. 9. DisCoverage exploration process with 3 robots

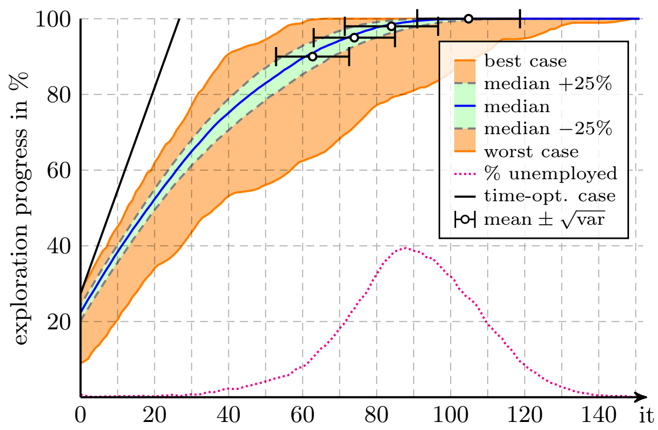

Fig. 10. Statistics of 1000 simulation runs for $N = 3$ robots

For clarity, only single-integrator dynamics and convex environments were handled. However, the proposed approach can be extended to passive and unicycle dynamics (Cortés et al., 2004; Bullo et al., 2009) as well as nonconvex environments with minor adjustments.

It is further noteworthy that the Voronoi partition is not necessarily optimal for the multi-robot exploration task, since unemployed robots do not contribute to the exploration. Therefore, finding an optimal partition in a distributed way for exploration is still an open problem.

REFERENCES

Bhattacharya, S., Michael, N., and Kumar, V. (2013). Distributed coverage and exploration in unknown nonconvex environments. In *Distributed Autonomous Robotic Systems*, volume 83 of *Springer Tracts in Advanced Robotics*, 61–75. Springer.

Bullo, F., Cortés, J., and Martínez, S. (2009). *Distributed Control of Robotic Networks*. Princeton University Press.

Burgard, W., Moors, M., Stachniss, C., and Schneider, F. (2005). Coordinated multi-robot exploration. *IEEE Transactions on Robotics*, 21(3), 376–386.

Cao, M. and Hadjicostis, C.N. (2003). Distributed algorithms for Voronoi diagrams and applications in adhoc networks. Technical report, University of Illinois at Urbana-Champaign, Urbana.

Cortés, J., Martínez, S., and Bullo, F. (2005). Spatially-distributed coverage optimization and control with limited-range interactions. *ESAIM, Control, Optimisation and Calculus of Variations*, 11(4), 691–719.

Cortés, J., Martínez, S., Karatas, T., and Bullo, F. (2004). Coverage control for mobile sensing networks. *IEEE Trans. on Robotics and Automation*, 20(2), 243–255.

Cortés, J., Martínez, S., Karatas, T., and Bullo, F. (2002). Coverage control for mobile sensing networks: variations on a theme. In *Proc. of the 10th Mediterranean Conference on Control and Automation*. Lisbon, Portugal.

de Berg, M., Cheong, O., van Kreveld, M., and Overmars, M. (2008). *Computational Geometry: Algorithms and Applications*. Springer.

Elfes, A. (1987). Sonar-based real-world mapping and navigation. *IEEE Journal of Robotics and Automation*, 3(3), 249–265.

Fabbri, R., da F. Costa, L., Torelli, J.C., and Bruno, O.M. (2008). 2D Euclidean Distance Transform Algorithms: A Comparative Survey. *ACM Computing Surveys*, 40(1), 1–44.

Fox, D., Ko, J., Konolige, K., Limketkai, B., Schulz, D., and Stewart, B. (2006). Distributed multirobot exploration and mapping. *Proceedings of the IEEE*, 94(7), 1325–1339.

Frank, S., Listmann, K., Haumann, D., and Willert, V. (2010). Performance analysis for multi-robot exploration strategies. In *Simulation, Modeling, and Programming for Autonomous Robots (SIMPAR 2010)*, 399–410. Springer.

Haumann, A.D., Listmann, K.D., and Willert, V. (2010). DisCoverage: A new paradigm for multi-robot exploration. In *Proc. of the IEEE International Conference on Robotics and Automation (ICRA)*, 929–934.

Haumann, D. (2013). DisCoverage Multi-Robot Exploration Framework. Software electronically available at `http://gitorious.org/discoverage`.

Haumann, D., Breitenmoser, A., Willert, V., Listmann, K.D., and Siegwart, R. (2011). DisCoverage for nonconvex environments with arbitrary obstacles. In *Proc. of the IEEE International Conference on Robotics and Automation (ICRA)*, 4486–4491.

Hussein, I. and Stipanovic, D. (2007). Effective coverage control for mobile sensor networks with guaranteed collision avoidance. *IEEE Transactions on Control Systems Technology*, 15(4), 642–657.

Khalil, H.K. (2001). *Nonlinear Systems*. Prentice Hall, 3rd edition.

Latombe, J.C. (1991). *Robot Motion Planning*. Kluwer Academic Publishers, Norwell, MA, USA.

LaValle, S.M. (2006). *Planning Algorithms*. Cambridge University Press.

Lozano-Pérez, T. and Wesley, M.A. (1979). An algorithm for planning collision-free paths among polyhedral obstacles. *Communications of the ACM*, 22(10), 560–570.

Martínez, S., Cortés, J., and Bullo, F. (2007). Motion coordination with distributed information. *IEEE Control Systems Magazine*, 27(4), 75–88.

Moravec, H.P. (1988). Sensor fusion in certainty grids for mobile robots. *AI Magazine*, 9(2), 61–74.

Pimenta, L.C.A., Schwager, M., Lindsey, Q., Kumar, V., Mesquita, R.C., and Pereira, G.A.S. (2008). Simultaneous coverage and tracking (scat) of moving targets with robot networks. In *Proc. of the 8th International Workshop on the Algorithmic Foundations of Robotics.*

Rooker, M. and Birk, A. (2007). Multi-robot exploration under the constraints of wireless networking. *Control Engineering Practice*, 15(3), 435–445.

Schwager, M., Rus, D., and Slotine, J.J. (2011). Unifying geometric, probabilistic, and potential field approaches to multi-robot deployment. *International Journal of Robotics Research*, 30(3), 371–383.

Sheng, W., Yang, Q., Tan, J., and Xi, N. (2006). Distributed multi-robot coordination in area exploration. *Robotics and Autonomous Systems*, 54(12), 945–955.

Udupa, S., of Technology. Division of Engineering, C.I., and Science, A. (1977). *Collision Detection and Avoidance in Computer Controlled Manipulators*. CIT theses. California Institute of Technology.

Wu, L., Puig, D., and García, M.A. (2010). Balanced multi-robot exploration through a global optimization strategy. *Journal of Physical Agents*, 4, 35–44.